Contrib Mineral Petrol (2003) 145: 752–764
DOI 10.1007/s00410-003-0478-6

ORIGINAL PAPER

Charles A. Geiger · Mathias Grams

Cordierite IV: structural heterogeneity and energetics of Mg–Fe solid solutions

Received: 22 November 2002 / Accepted: 23 April 2003 / Published online: 8 August 2003

Abstract The local structural heterogeneity and energetic properties of 22 natural Mg–Fe cordierites, ideal formula $(Mg,Fe)_2Al_4Si_5O_{18}{\cdot}x(H_2O,CO_2)$, were investigated at length scales given by powder infrared spectroscopy (IR) and also by published electronic absorption spectra. The studied samples have iron mole fractions from $X_{Fe} = 0.06$ to 0.82 and cover most of the Mg–Fe cordierite binary. Variations in wavenumbers and line widths of the IR bands were determined as a function of composition. Most modes shift linearly to lower wavenumbers with increasing X_{Fe}, except those at high wavenumbers located between 900 and 1,200 cm^{-1}. They are vibrations that have a large internal $(Si,Al)O_4$ character and are not greatly affected by Mg–Fe exchange on the octahedral site. The lower wavenumber modes can be best characterized as lattice vibrations having mixed character. The systematics of the wavenumber shifts suggest small continuous variations in the "average" cordierite structure with Mg–Fe exchange and are consistent with an ideal volume of mixing, $\Delta V^{mix} = 0$, behavior (Boberski and Schreyer 1990). IR line broadening was measured using the autocorrelation function for three wavenumber regions in order to determine the range of structural heterogeneity between roughly 2 and 100 Å (0.2–10.0 nm) in the solid solution. In order to do this, an empirical correction was first made to account for the effect that small amounts of channel Na have on the phonon systematics. The results show that between 1,200 and 540 cm^{-1} the line widths of the IR bands broaden slightly and linearly with increasing X_{Fe}. Between 350 and 125 cm^{-1} nonlinear behavior was observed and it may be related to dynamic effects. These results suggest minimal excess elastic enthalpies of mixing for Mg–Fe cordierite solid solutions. Channel Na should affect measurably the thermodynamic properties of natural cordierites as evidenced by variations in the IR spectra of Na-containing samples. Occluded H_2O (Class I) and CO_2 should have little interaction with the framework and can be considered nearly "free" molecules. They should not give rise to measurable structural heterogeneity in the framework. The contribution of the crystal field stabilization energy (CFSE) of octahedral Fe^{2+} to the energetics of Mg–Fe cordierites was also investigated using published electronic absorption spectra (Khomenko et al. 2001). Two bands are observed between 8,000 and 10,500 cm^{-1} and they represent electronic dd-excitations of octahedral Fe^{2+} derived from the $^5T_{2g} \rightarrow {}^5E_g$ transition. They shift to higher wavenumbers with increasing X_{Mg} in cordierite. An analysis gives slightly asymmetric excess $-\Delta$CFSE across the Mg–Fe cordierite join with a maximum of about −550 J/mole towards iron-rich compositions.

Editorial responsibility: J. Hoefs

C. A. Geiger (✉) · M. Grams
Institut für Geowissenschaften,
Christian-Albrechts-Universität zu Kiel,
Olshausenstr. 40, 24098 Kiel, Germany
E-mail: chg@min.uni-kiel.de

Introduction

Cordierite is a common metamorphic mineral typically found in low to medium pressure amphibolite and granulite facies rocks of appropriate composition. Natural cordierites are magnesium–iron solid solutions with the ideal formula $(Mg,Fe)_2Al_4Si_5O_{18}{\cdot}x(H_2O,CO_2)$. Most crystals are magnesium rich in composition and crystals have been found closely approaching the Mg end member (Pryce 1973). Iron-rich cordierites are rare and the most iron-rich sample ($X_{Fe} \approx 0.82$) reported to date comes from a pegmatite (Stanek and Miskovsky 1964). A determination of the thermodynamic properties of Mg–Fe cordierite solid solutions is important for a variety of petrologic applications, because cordierite-bearing assemblages are often used to determine metamorphic phase relations (e.g., Pattison et al. 2002). However, little is understood about the energetics associated with the Mg–Fe exchange, which is fundamental and found in many rock-forming silicates.

Because of the similarity in the ionic radii of Mg^{2+} and Fe^{2+} (Shannon 1976), it is often assumed that elastic strain arising from their mixing should be minimal and Mg–Fe silicate solid solutions should show ideal thermodynamic behavior or nearly so. This has been discussed many times (e.g., Mueller 1962; Kerrick and Darken 1975; Thompson 1976; Geiger 2001). However, there are some Mg–Fe silicates such as olivine (Wood and Kleppa 1981; Kojitani and Akaogi 1994), for example, where nonideality could be present and a full quantitative understanding of the thermodynamic behavior associated with Mg–Fe exchange in silicates is not at hand. In addition to elastic strain energies, magnetic and electronic effects associated with the transition metal Fe^{2+} can also influence the macroscopic properties and much work needs to be done to determine their contribution to the total energetics of a system.

Structural changes accompanying Mg–Fe exchange in cordierite were determined in several single-crystal X-ray diffraction studies (Wallace and Wenk 1980; Armbruster 1985; Malcherek et al. 2001). Thus, the structure has been well described over long length scales (i.e., tens to several hundred nanometers). On the other hand, there has been very little done in terms of investigating the cordierite structure over shorter length scales between about 1 and 10 nm using infrared (IR) and Raman methods. Most vibrational spectroscopic measurements have concentrated on investigating the occluded H_2O and CO_2 molecules (e.g., Kolesov and Geiger 2000 and references therein) and little work has been done on investigating the phonons associated with the framework for solid-solution compositions. Langer and Schreyer (1969) undertook some of the first powder IR measurements in a study of synthetic Mg cordierite to characterize Al/Si ordering (see also Güttler et al. 1989). Boberski and Schreyer (1990) presented IR spectra of three synthetic intermediate Mg–Fe cordierites. No IR or Raman study has been undertaken to investigate directly the nature of Mg–Fe mixing. The time is ripe for such an investigation, because it has been shown that vibrational spectroscopy is a useful tool in describing ordering processes, phase transitions and local structural changes resulting from solid solution (see for a review Salje and Bismayer 1997). This general type of study has been termed hard mode spectroscopy (HMIRS when the IR-active phonons are investigated) and a number of binary silicate solid solutions have been investigated including alkali and plagioclase feldspars, clinopyroxenes, garnets, and orthopyroxenes (Zhang et al. 1996; Boffa Ballaran et al. 1998, 1999; Atkinson et al. 1999; Tarantino et al. 2002). The investigations have shown that microscopic-nanoscopic structural heterogeneities can be characterized from a precise determination of phonon band energies and their associated line widths in vibrational spectra. Variations in line widths of IR bands contain information on the range of structural heterogeneities over different length scales given by the IR-active phonons. Their determination in low symmetry structures with large unit cells is not an easy task, because the IR spectra often contain a large number of strongly overlapped bands. Here, the autocorrelation function is used, because it provides a means for determining their line widths independent of their shape or degree of overlapping (Salje et al. 2000). It was shown for pyroxene, feldspar, and garnet solid solutions that changes in line widths correlate well with the enthalpy of mixing determined by calorimetry (Boffa Ballaran et al. 1998, 1999; Atkinson et al. 1999). This means that an analysis of phonon spectra can provide information on macroscopic thermodynamic mixing properties (Carpenter and Boffa Ballaran 2001), which are difficult and time consuming to measure directly and for which calorimetric data often do not exist (Geiger 2001).

The aim of this study is to investigate local structural heterogeneity at length scales determined by IR-active phonons and to analyze the thermodynamic mixing properties and energetics of natural Mg–Fe cordierite solid solutions. There are few to no calorimetric measurements or phase equilibrium experiments that bear directly on this problem and, therefore, an understanding of the thermodynamics of cordierite is poor. An analysis of the crystal field stabilization energies of Fe^{2+} across the Mg–Fe join is also made in order to document their contribution to the energetics of the cordierite system.

Structure, lattice dynamics and chemistry

Cordierite is a framework silicate (Gibbs 1966) that has six-membered rings consisting of corner-sharing $(Si/Al)O_4$ tetrahedra that are cross-linked by octahedra and other tetrahedra in the (001) plane forming a three-dimensional framework (Fig. 1). The rings are stacked over one another producing infinite channels running parallel to the *c*-axis and they form "bottle necks" with a free diameter of about 2.6 Å in which alkali cations, such as Na, can be incorporated (Armbruster 1982, 1986). In the cavities (about 5.5 by 6.0 Å in size) between the "bottle necks", various molecules (e.g., H_2O, CO_2) and neutral atoms (Ar) can be found. The rings in "low" cordierite contain two $T_2$6 and four $T_2$3 and $T_2$1 tetrahedra, while the $T_1$1 and the $T_1$6 tetrahedron cross-link the rings together. In nature most cordierites, that is those of regional and contact metamorphic rocks, have an ordered (Si, Al) distribution. This leads to an orthorhombic unit cell of space group of *Cccm* (Gibbs 1966). In "high" cordierite, called indialite, Si and Al are statistically distributed over the T_1 and T_2 sites. High cordierite crystallizes in space group *P6/mcc* and is seldom found in nature with the exception, for example, in high-temperature geologic environments such as in fused sediments (Miyashiro and Iiyama 1954).

The total irreducible representation at the Γ-point for "low" cordierite with $Z = 4$ is given as follows (White 1974):

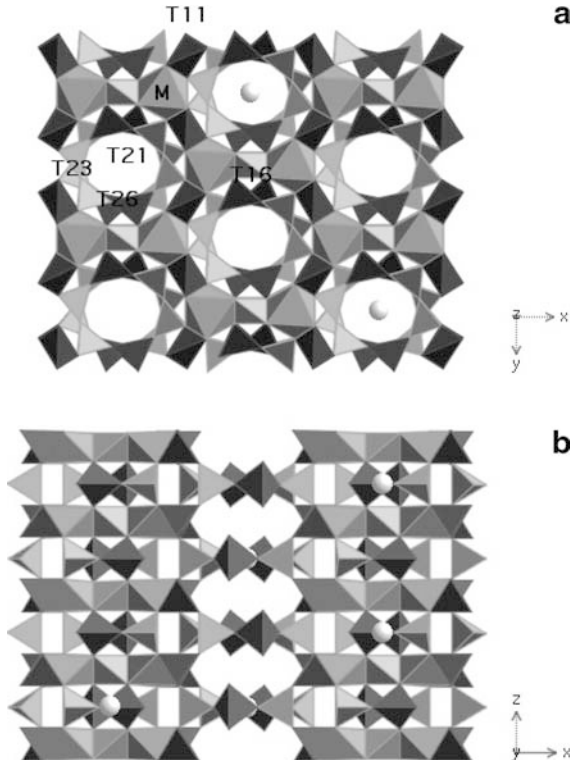

Fig. 1 Structure of low cordierite. Al occupies the *tetrahedra in dark gray*, whereas Si occupies the *lighter* ones. The *spheres* represent alkali cations (Na, K) located in the six-membered rings of $(Si/Al)O_4$ tetrahedra and their concentration is variable. The different crystallographic cation sites are labeled

$$\Gamma = 23A_g + 25B_{1g} + 20B_{2g} + 19B_{3g} + 18B_{1u} + 25B_{2u} + 24B_{3u} + 17A_u. \quad (1)$$

The *ungerade* B symmetry modes, except for three B_{iu}, where $i = 1$, 2, or 3, acoustic modes, are IR active giving a total of 64. There has been little experimental or computational work done to assign the different modes to atomic or polyhedral motions.

The chemistry of natural cordierites is now well understood. With respect to the cation polyhedra, the elements Li and Mn^{2+} can substitute for Mg and Fe^{2+} on the octahedral M site. The large $T_1 1$ site has mostly Al^{3+}, but it can also contain Be (Armbruster 1986) as a result of solid solution toward a beryl component (Newton 1966) or through coupled substitutions (Cerny and Povondra 1966). Geiger et al. (2000a) showed that small amounts (maximum of about 10 at%) of Fe^{2+} can be found on $T_1 1$, and Fe^{3+} also occurs there but in very small concentrations (Geiger et al. 2000b). Minor amounts of Mg may also be found on this site (Malcherek et al. 2001). Alkali cations, primarily Na and K, can be found in the center of the six-membered rings (Armbruster 1986; Schreyer et al. 1990). Thus, a generalized chemical formula for most natural cordierites with major and minor elements can be written as: $^{Ch}[Na, K]_y(Mg, Fe^{2+}, Mn^{2+}, Li)_2(Al, Be, Mg, Fe^{2+}, Fe^{3+})_4Si_5O_{18}\cdot x^{Ch}[H_2O, CO_2]$, where y and $x < 1.0$. There can be variations in the Al:Si ratio from the ideal value of 4:5 and Fe-rich crystals show less order on T_1than Mg-rich crystals (Malcherek et al. 2001). This arises from coupled substitutions associated with the incorporation of alkali cations in the channels and Li on the octahedral site, for example, which then require charge balance through the crystallographic framework sites (Schreyer 1985). It should be noted that cordierite can contain measurable amounts of Na_2O up to 6.5 wt% (Fuchs 1969), but in most terrestrial cordierites the concentration is seldom greater than 1.5 wt%. Its incorporation can be the result of different coupled substitutions such as $Na^+ + Be^{2+} \rightarrow Al^{3+}$, $Na^+ + Li^+ \rightarrow Fe^{2+}/Mg$, or $Na^+ + Fe^{2+} \rightarrow Al^{3+}$ typically giving between 0.01 and 0.35 Na cations p.f.u. (Cerny and Povondra 1966; Schreyer 1985; Armbruster 1986; Geiger et al. 2000a; Malcherek et al. 2001).

Experimental methods

Powder IR measurements were undertaken on 22 natural cordierites. Many of the samples have been used in other spectroscopic studies and are described therein (Geiger et al. 2000a, 2000b; Kolesov and Geiger 2000; Khomenko et al. 2001) and they can be considered well characterized. In those cases where no single crystal was available, cordierite was obtained from the rock assemblages by magnetic separation and hand picking. The major elements were measured by electron microprobe analysis (Table 1) on crystal separates embedded in epoxy holders (a discussion of microprobe and ion probe methodologies including both the major and light elements, i.e., B, Be, and Li, will be given in more detail in another report considering the chemistry of natural cordierites). The iron mole fraction used in following discussions and figures is calculated as $X_{Fe} = (Fe^{2+} + Mn^{2+})/(Fe^{2+} + Mn^{2+} + Mg)$, because Mn^{2+} is similar in size to Fe^{2+} and because it is also a transition metal. The effect of tetrahedral Fe^{2+} and Mg on this ratio is minor and offsetting and is not considered.

For the HMIRS measurements care was taken to exclude samples that had inclusions or showed signs of alteration (e.g., pinite). Several tens of milligrams of cordierite were ground by hand in an agate mortar to obtain a fine and homogeneous size fraction. This is important for quantitative HMIRS measurements (e.g., Salje and Bismayer 1997; Boffa Ballaran et al. 1999). For measurements in the MIR range, 0.7 mg of cordierite together with 200 mg of KBr were pressed into disks under vacuum. Polyethylene was used for the FIR measurements with a matrix to sample ratio of 40 to 2 mg. The preparation of the disks requires care, because small variations in the grain distribution size or differences in sample weight lead to small but measurable differences in line widths. The measurements were done using a Bruker 66 v/s FTIR spectrometer. The MIR spectra were collected in the wavenumber range 350 to 4,000 cm^{-1} at a resolution of 2 cm^{-1} and the FIR spectra at the same resolution between 50 and 500 cm^{-1}. In the MIR region a KBr and in the FIR a Mylar 6 beam splitter was used. The resulting spectra were made by collecting and averaging 512 interferometer scans using a DTGS detector.

Results

Description of IR spectra

The powder spectra of representative cordierites of different X_{Fe} are shown between 70 and 1,300 cm^{-1} in

Table 1 Electron microprobe results for the 22 studied cordierite samples. Chemical formulas are normalized to 18 oxygens. $X_{Fe} = (Fe + Mn)/(Fe + Mn + Mg)$

Sample no.	1	2	3	4	4	6	7	8	9	10	11	12	13	14	15	16	17	18	19	20	21	22[a]
SiO_2	50.06	49.02	50.19	49.56	50.00	50.05	48.89	49.82	50.25	49.54	49.19	50.06	48.57	49.64	49.08	49.12	48.32	47.53	46.90	47.11	45.71	48.37
Al_2O_3	32.71	33.32	33.96	33.70	33.32	33.33	33.63	33.76	33.08	32.95	33.29	33.39	33.15	33.28	33.01	32.96	32.84	32.39	32.14	31.66	31.61	30.86
MgO	13.14	12.83	12.33	12.32	12.00	12.00	12.13	11.74	11.99	10.96	10.78	10.43	10.73	9.93	9.60	8.67	7.86	7.73	5.60	3.32	2.14	8.86
FeO	1.57	2.33	2.31	2.75	2.70	2.71	2.63	3.05	3.15	4.55	4.50	4.89	5.02	5.87	6.13	7.98	9.01	9.56	13.10	16.84	16.80	6.66
MnO	0.02	0.02	0.02	0.04	0.04	0.04	0.03	0.04	0.03	0.05	0.07	0.22	0.22	0.06	0.04	0.05	0.24	0.15	0.07	0.10	0.66	0.33
Na_2O	0.34	0.32	0.22	0.34	0.23	0.52	0.20	0.10	0.03	0.07	0.25	0.17	0.28	0.07	0.09	0.08	0.44	0.44	0.04	0.08	0.58	1.41
Total	97.84	97.84	99.07	98.71	98.29	98.65	97.51	98.51	98.53	98.12	98.08	99.16	97.97	98.85	97.95	98.86	98.71	97.80	97.89	99.11	97.50	96.53
Si	5.03	4.95	4.99	4.96	5.02	5.01	4.95	5.00	5.04	5.021	4.99	5.03	4.96	5.02	5.02	5.02	4.99	4.96	4.96	5.00	4.97	5.07
Al	3.87	3.96	3.98	3.98	3.94	3.93	4.01	3.99	3.91	3.936	3.98	3.95	3.99	3.97	3.98	3.97	4.00	3.99	4.01	3.96	4.05	3.81
Mg	1.97	1.93	1.83	1.84	1.80	1.79	1.83	1.75	1.79	1.656	1.63	1.56	1.63	1.50	1.46	1.32	1.21	1.20	0.88	0.53	0.35	1.38
Fe	0.13	0.20	0.19	0.23	0.23	0.23	0.22	0.26	0.26	0.385	0.38	0.41	0.43	0.50	0.52	0.68	0.78	0.83	1.16	1.50	1.53	0.58
Mn	0.00	0.00	0.00	0.00	0.00	0.00	0.00	0.00	0.00	0.001	0.01	0.02	0.02	0.01	0.00	0.00	0.02	0.01	0.01	0.01	0.06	0.03
Na	0.06	0.06	0.04	0.07	0.04	0.10	0.04	0.02	0.01	0.013	0.05	0.03	0.06	0.01	0.02	0.02	0.04	0.09	0.01	0.02	0.12	0.29
X_{Fe}	0.06	0.09	0.10	0.11	0.11	0.11	0.11	0.13	0.13	0.19	0.19	0.22	0.22	0.25	0.26	0.34	0.40	0.41	0.57	0.74	0.82	0.31

[a]0.67 BeO, 0.23 Li_2O (wt%) from Armbruster and Irouschek (1983)

Fig. 2. The final spectra were produced by merging the MIR and FIR regions together between 350 and 500 cm^{-1} where they overlap. Cordierite's IR spectrum is characterized by several band "systems" containing a number of overlapping modes. Moving from high to low wavenumbers two major band envelopes centered around 1,175 and 950 cm^{-1} are visible. They are followed by a strong mode at about 750 cm^{-1}, having a shoulder on its low energy side, and then several weak modes between 700 and 625 cm^{-1}. Towards lower wavenumbers a band triplet occurs at about 575 $cm^{-1}$and then a wide band envelope occurs between 500 and 300 cm^{-1}. The modes in the FIR region between 300 and 100 cm^{-1} are the weakest in the spectra and are present up to the low energy flank of the envelope between 500 and 300 cm^{-1}. The mode wavenumbers were determined by measuring the first and second derivatives of the bands in the spectra. Measurable changes in the mode energies occur as a result of Mg–Fe substitution (cf. Boberski and Schreyer 1990) and this is especially true for those between 500 and 700 cm^{-1} and 50 and 300 cm^{-1}. Generally, the line widths become broader and their intensities decrease with increasing X_{Fe}.

No lattice dynamic calculations or empirically based spectroscopic investigations on cordierite have been made in order to assign completely the IR modes. Some of the first simple mode assignments derive from the study of Langer and Schreyer (1969) and we adopt their notation for the description of our spectra. They assigned the different E and F modes at the highest wavenumbers to tetrahedral stretching vibrations. Boberski and Schreyer (1990), citing the work of Plyusina et al. (1981), consider the band systems A, E, and F to represent "valent asymmetric oscillation and deformation oscillation of the Si–O–Si bond". Band system D is typical of ring silicates and "corresponds to valent symmetric oscillation of the Si–O–Si bond". Bands C1, C2, and B1 were proposed to be "oscillations of six-coordinated cation groups." A more definitive lattice dynamic analysis with quantitative band assignments is lacking. It must be stressed that mode coupling and mixing are probably well developed (see Geiger and Kolesov 2003). We emphasize, though, that a lattice dynamic treatment is not a goal of our study, nor is it necessary for the conclusions made below.

Mode energy shifts as a function of composition

The two highest wavenumber modes show only small changes in their energies as a function of composition (Fig. 3). Modes E1 and E2 shift slightly to higher wavenumbers with increasing X_{Fe}, opposite to the general trend of the other modes. Between 800 and 250 cm^{-1}all modes, except A1, decrease in wavenumber with increasing X_{Fe}. Due to band overlap in this region, some of these bands are combinations and it is difficult to determine exactly the mode energy of the different components. Modes C1 and C2 decrease in intensity

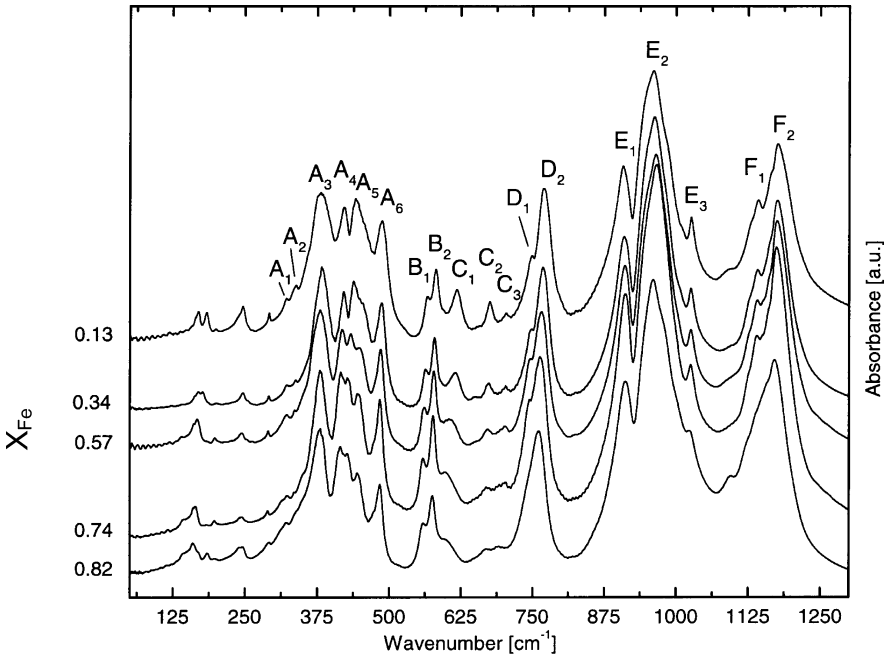

Fig. 2 Infrared powder absorption spectra between 50 and 1,300 cm^{-1} for selected Mg–Fe cordierite solid solutions. Band notation from Langer and Schreyer (1969)

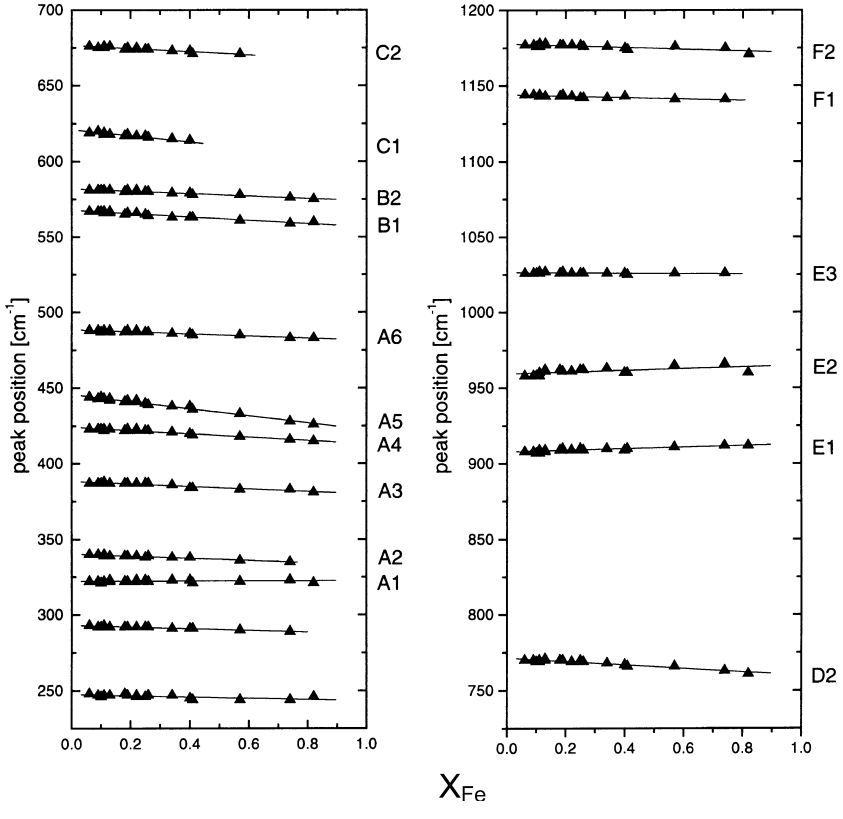

Fig. 3 Wavenumber shifts of the IR phonons as a function of X_{Fe}. **a** Between 225 and 700 cm^{-1}; **b** between 750 and 1,200 cm^{-1}

with increasing X_{Fe} and C1 moves towards B2 until they overlap. Therefore, the position of C1 cannot be determined quantitatively at large X_{Fe}. The different bands of the A-envelope show measurable shifts with changing composition. Band A5 splits with increasing X_{Fe}.

In the FIR region a band around 185 cm^{-1} occurs in Mg-rich compositions and it merges and shifts to lower wavenumbers with increasing X_{Fe} (Fig. 4). At compositions greater than $X_{Fe} > 0.4$, the two bands are overlapped and cannot be easily differentiated. This and increased line broadening make a precise determination of the mode energies and line widths in iron-rich cordierites difficult. We do not, therefore, use these bands in the following analysis. The wavenumber shifts

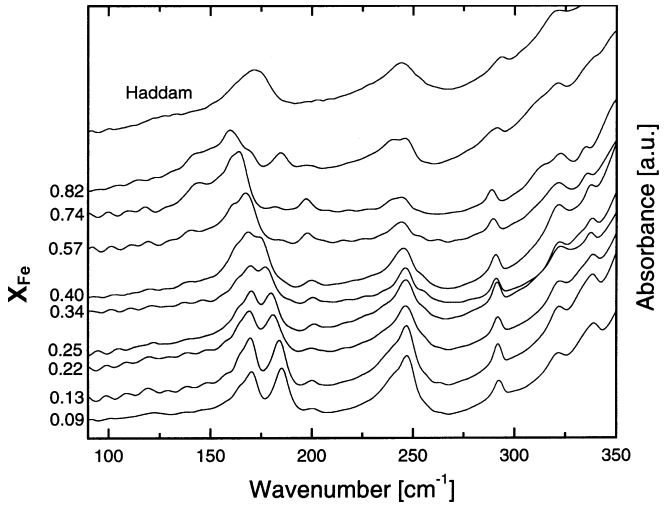

Fig. 4 FIR powder absorption spectra in the wavenumber region 100–350 cm^{-1} for a series of Mg–Fe cordierite solid solutions The Na(Be)-rich cordierite no. 22 (from Haddam, USA) is shown *above*

Table 2 Coefficients and R values resulting from fitting the data shown in Fig. 3 where band wavenumber (cm^{-1}) = mX_{Fe} + b

Band	b (in cm^{-1})	m (in cm^{-1}) ($\pm$0.5 cm^{-1})	R
–	247	–4.2(9)	0.74
–	293	–5.4(5)	0.95
A1	322	0.3(6)	0.14
A2	340	–7.1(5)	0.96
A3	388	–8.4(7)	0.95
A4	424	–11.0(6)	0.98
A5	445	–23.3(7)	0.99
A6	488	–7.0(5)	0.96
B1	568	–12.4(5)	0.98
B2	581	–8.0(4)	0.98
C1	621	–20.5(22)	0.92
C2	676	–10.4(11)	0.92
D2	771	–11.6(8)	0.96
E1	907	5.2(7)	0.88
E2	959	5.7(19)	0.57
E3	1,026	–1.2(7)	0.41
F1	1,144	–4.7(8)	0.84
F2	1,177	–5.8(10)	0.80

of the different bands shown in Fig. 3 were fitted as a function of composition with a linear equation, $y = m \cdot X + b$, and the resulting coefficients for the fits are given in Table 2.

It should be noted that some modes associated with the cordierite sample no. 22, which has a high sodium and beryllium content (Table 1), differ measurably from the other samples. Therefore they are not plotted in Fig. 3. Its bands, especially in the envelope F, show lower wavenumbers compared to Na-poor cordierites. All of its other MIR modes lie at higher wavenumbers in comparison to those of Na-poor cordierites, for example band A5 (Fig. 5). In order to determine the effect of sodium on mode energies for the different samples, the wavenumbers of bands E2 and F2 were recorded as a function of Na_2O content (Fig. 6). They should be most

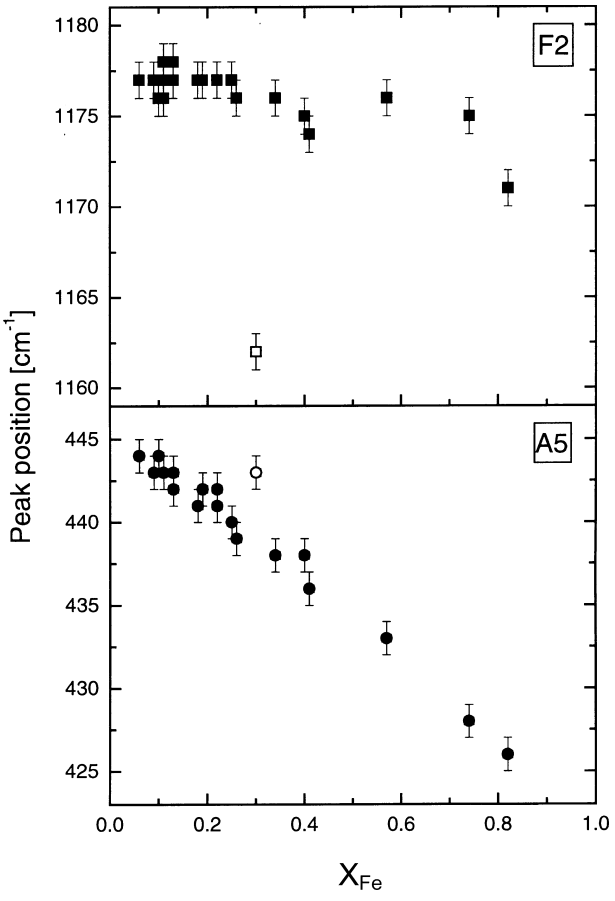

Fig. 5 Peak shifts of bands F2 and A5 as a function of X_{Fe}. The *open symbols* indicate the Na(Be)-rich cordierite no. 22

affected by Na, because they have a strong $Si(Al)O_4$ vibrational character. For band F2 there does not appear to be major variations, but E2 shifts to slightly lower wavenumbers with increasing Na_2O content.

Band line widths as function of composition

The strong overlapping of bands and difficulties in determining precisely the baseline in the spectra make a quantitative determination of line widths difficult using traditional peak fitting methods that involve fitting individual Lorenzian or Gaussian curves. To circumvent these problems, the autocorrelation function was introduced to determine subtle energy shifts and changes in line widths for complicated vibrational spectra (Salje et al. 2000), and it has been applied in the study of different solid solutions (Zhang et al. 1996; Boffa Ballaran et al. 1998, 1999; Atkinson et al. 1999; Tarantino et al. 2002). For its application, knowledge of the exact number, shape or position of the different individual bands is not necessary. It is given as:

$$\mathrm{Corr}(g, \bar{v}') = \int_{-\infty}^{+\infty} g(\bar{v} + \bar{v}')g(\bar{v})d\bar{v}, \quad (2)$$

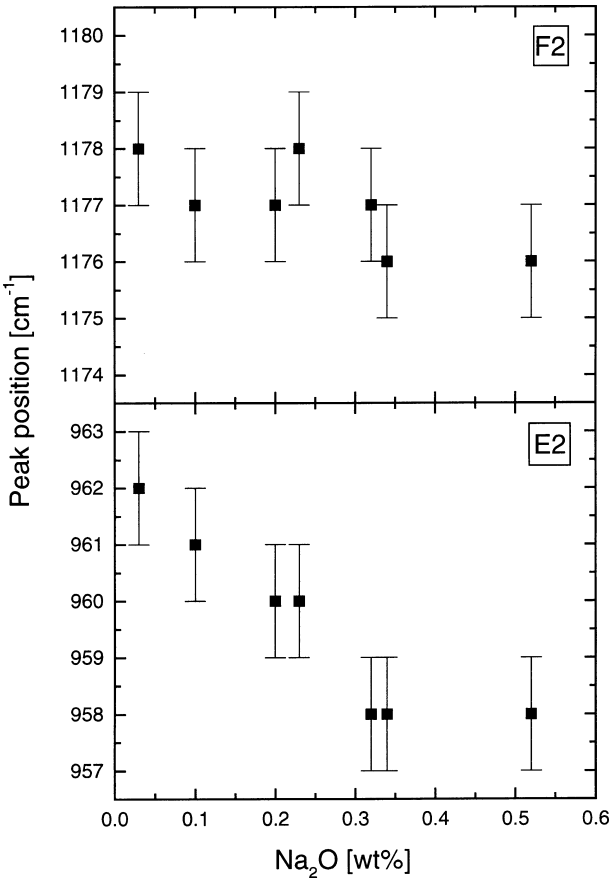

Fig. 6 Wavenumber of bands F2 and E2 as a function of the wt% of Na_2O. All samples have $X_{Fe} = 0.09–0.13$

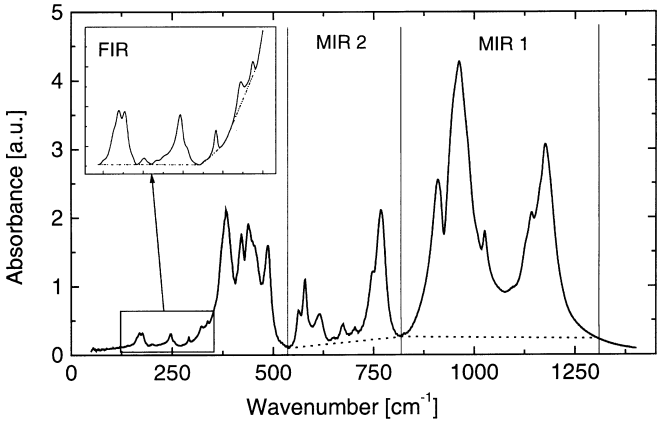

Fig. 7 Division of the IR spectra in three wavenumber regions used for the autocorrelation determinations. The *dotted lines* show the assumed baselines

and it can be used to determine line widths. Corr(g, $\bar{\nu}'$) is defined as the product of the primary spectrum, $g(\bar{\nu})$, with $g(\nu + \bar{\nu}')$, that is after a shift in frequency of $\bar{\nu}'$. One obtains through this treatment (e.g., see Boffa Ballaran et al. 1999; Salje et al. 2000) a value for Δ_{corr}, which is proportional to the average line

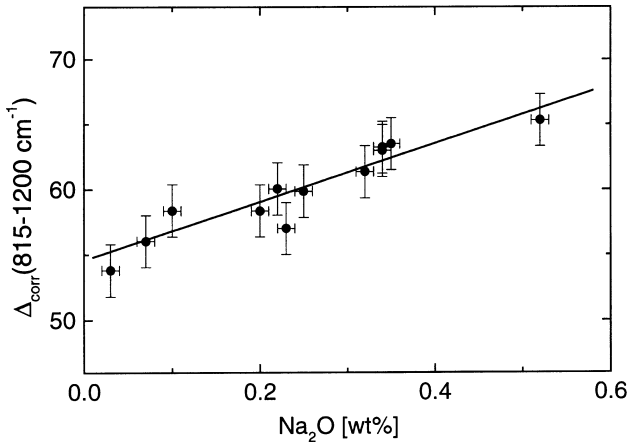

Fig. 8 Δ_{corr} values in [cm^{-1}] as a function of Na_2O concentration for cordierites with $X_{Fe} = 0.06–0.19$

widths for a chosen wavenumber region of a spectrum. Figure 7 shows a representative powder IR spectrum of cordierite, and the three different wavenumber regions for which Corr(g, $\bar{\nu}'$) was determined. For the two MIR regions a linear baseline was subtracted from the spectra prior to fitting. In the FIR region, a background correction termed the "rubber band method" is more suitable. An analysis shows that, especially in the MIR 1 region, the Na-rich cordierites have larger Δ_{corr} values relative to Na-poor samples. Therefore, we determined the line widths in this region for 11 samples as a function of Na_2O content (Fig. 8). The results show a linear increase in Δ_{corr} with increasing Na. Because we are interested primarily in line broadening associated with Mg–Fe exchange, the Δ_{corr} values of the different cordierites were then corrected for their respective Na contents. Figure 9a, b shows the data for the MIR1 region both before and after this procedure. Na-rich cordierite no. 22, for example, plots on a straight line with the Na-poor samples after this correction (Fig. 9b) and, therefore, we think this empirical procedure has validity. For the FIR range a similar correction to the Δ_{corr} values was undertaken. In the MIR 2 range no correction was necessary, because the Na content does not measurably affect the line widths.

The final Δ_{corr} values show a linear increase with increasing X_{Fe} from about 55 to 65 cm^{-1} for the region MIR 1 and about 22 to 30 cm^{-1} for the region MIR 2 and a nonlinear deviation from linearity in the FIR region (Fig. 10). This deviation can be fit with a second-order polynomial function giving Δ_{corr} (cm^{-1}) = 6.6(3) + 16(2)·X_{Fe} − 13(2)·X^2_{Fe}. For cordierite no. 22, where strong line broadening in the FIR region is present, the Δ_{corr} values are not plotted. Those of cordierite no. 2 are, even after a correction for Na, shifted to slightly higher values in comparison to the general trend arising from Mg–Fe exchange. The data indicate that Δ_{corr} values for Mg-rich versus Fe-rich cordierite are measurably different.

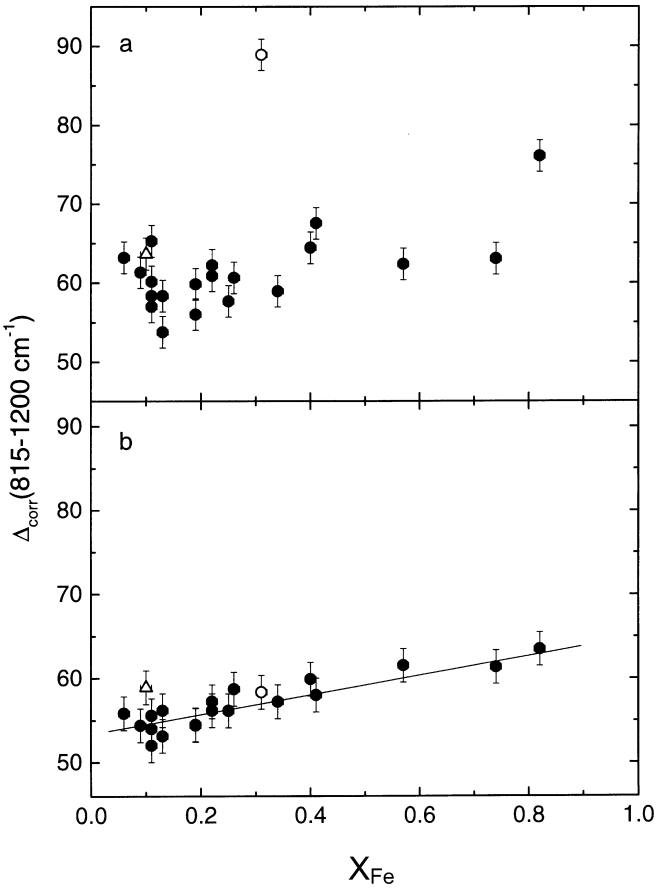

Fig. 9 Average line widths (Δ_{corr} in [cm^{-1}]) for the MIR 1 range as a function of X_{Fe}. **a** Uncorrected and **b** corrected for Na content. The *open circle* belongs to sample no. 22 and the *open triangle* to sample no. 2

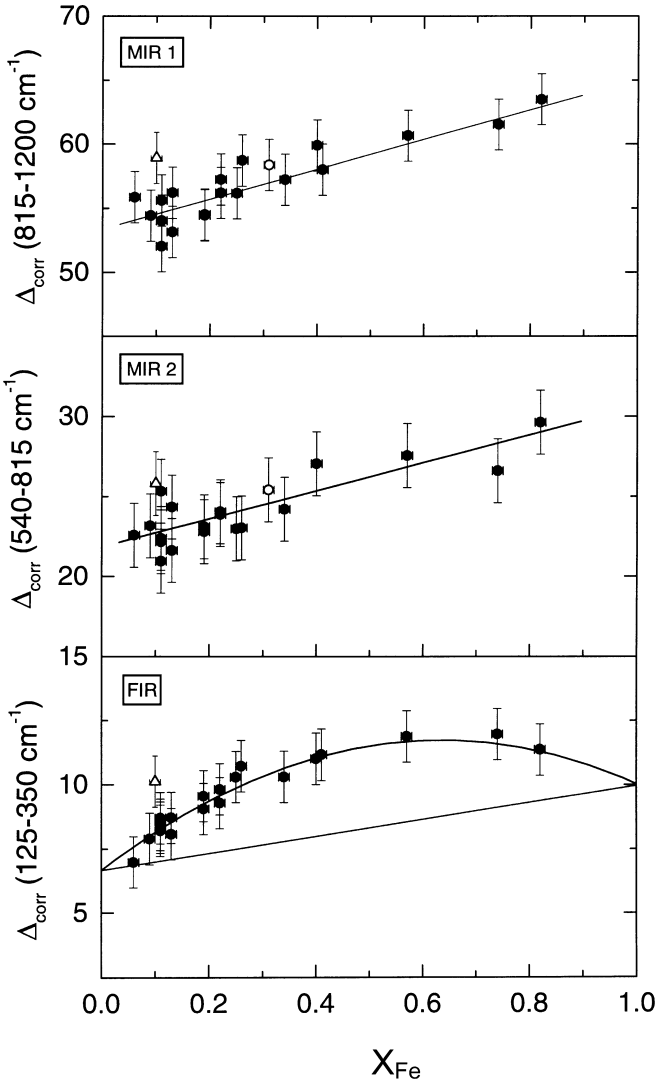

Fig. 10 Average line widths (Δ_{corr} in [cm^{-1}]) as a function of X_{Fe} in three different wavenumber regions. *Open circles* represent sample no. 22 and *open triangles* sample no. 2. The MIR 1 and FIR ranges were corrected for the Na content

Discussion

Crystal chemistry and framework distortion

In cordierite Mg–Fe exchange primarily takes place on the single octahedral M-site (Fig. 1). With increasing Fe-content, the M-site volume increases by about 5% from a nearly end member Mg cordierite with $X_{Fe} = 0.04$ to an iron-rich cordierite with $X_{Fe} = 0.82$ (11.8 vs 12.4 Å^3) as shown by X-ray diffraction results (Hochella et al. 1979) and is associated with a linear variation in the mean M–O bond length from about 2.105 to 2.160 Å (Wallace and Wenk 1980; Armbruster 1985; Malcherek et al. 2001). The volumes of the tetrahedra, in contrast, show no major variations. The cordierite framework responds to this octahedral volume change in various ways, as has been thoroughly discussed in the literature. Summarizing here, the mean T–O bond lengths of the ring tetrahedra do not change, while those of the distorted edge-shared $T_1$1 site decrease slightly with increasing X_{Fe} (from about 1.756 to 1.748 Å). Wallace and Wenk (1980) showed that with increasing X_{Fe} the rings move away from one another causing an increase in the *a* and *b* cell dimensions, while *c* decreases slightly. There is also a slight rotation (less than 0.5°) of neighboring overlying six-membered rings in opposite directions (Wallace and Wenk 1980; Armbruster 1985). The (Si/Al)–O bond lengths of the tetrahedra of the ring are not strongly affected by Mg–Fe exchange, but $T_1$1 and $T_1$6 become more distorted. All of these mechanisms appear to be important in relieving local strain in the framework resulting from the Mg–Fe exchange. One can conclude that the X-ray results, reflecting the average static structure, show small continuous variations in the framework with no abrupt changes or discontinuities.

In terms of lattice dynamics, it has been shown that the behavior of rigid-unit modes (RUMs) offers a sensitive measure of the structural variations and the type of distortions that can occur in silicates (Hammonds et al. 1996). RUMs can be considered as low energy vibrations that propagate through a structure without

causing any distortion of the tetrahedra. It has been shown that a number of "true" framework silicate structures (i.e., quartz, cristobalite, feldspar) contain RUMs and cordierite has similarities to this group. It was shown, for example, that the cordierite framework has enough degrees of freedom to adjust to structural changes through rigid polyhedral rotation, and a number of RUMs have been calculated (Hammonds et al. 1996). This suggests that the energies associated with internal $(Si/Al)O_4$ vibrations should not be greatly affected by the octahedral Mg–Fe exchange. Thus, Mg–Fe mixing in cordierite will be reflected quite differently in phonon spectra than the case for Mg–Fe mixing in garnet, for example. In garnet there are no RUMs and cation substitution on the dodecahedral X-site results in distortion of the SiO_4 tetrahedra (Hammonds et al. 1998).

Local structural heterogeneity and strain

The largest wavenumber shifts in Mg–Fe cordierites should be related to phonons with significant octahedral character, such as those represented by the bands C1 and C2 and A4 and A5 that decrease measurably with increasing X_{Fe}. We were not able to discern any overt indications for two-mode behavior (White 1974), which might be expected considering the large mass difference between Fe and Mg. It should also be stressed that any small variations from linearity (i.e., several wavenumbers) in mode energies were not possible to discern, because of the compositional and structural complexity inherent to the natural samples used. Information about the macroscopic volume of mixing behavior should be reflected in the phonon wavenumber systematics, whereby variations should reflect average local structural heterogeneities in the solid solution. In the case of strictly binary garnet solid solutions, for example, small nonlinear wavenumber shifts have been observed for certain IR modes and they can be correlated to the volume of mixing behavior (Geiger et al. 1989; Boffa Ballaran et al. 1999). Mg–Fe (almandine–pyrope) garnets, for example, have an ideal volume of mixing (i.e., $\Delta V^{mix} = 0$) and here the different IR phonon energies vary linearly as a function of garnet composition. For cordierite, the linear wavenumber shifts of all the IR modes (Fig. 3) suggest that the average cordierite structure varies in a continuous and linear manner upon Mg–Fe exchange. No major structural breaks occur at the microscopic or nanoscopic scale. This behavior is reflected further in the ideal volumes of mixing measured for synthetic $(Mg,Fe)_2Al_4Si_5O_{18}{\cdot}x(H_2O)$ solid solutions (Boberski and Schreyer 1990).

The solid-solution process must give rise to local structural distortions and thus, unlike end member composition crystals, there will be structural heterogeneity that generates elastic strains. Local phonons arise from the structural heterogeneity and line broadening will follow (White 1974). As discussed by Carpenter and Boffa Ballaran (2001), phonon length scales are not known precisely, but should vary with $1/\omega$, where ω is the wavenumber. They give length scales of ~2–5 Å around 1,500 cm^{-1}, ~6–15 Å around 500 cm^{-1} and ~60–150 Å around 50 cm^{-1}. The Δ_{corr} results on cordierite, which give a measure of line broadening, show a linear increase between 540 and 815 cm^{-1} and between 815 and 1,200 cm^{-1} with increasing X_{Fe} (Fig. 10). A possible explanation for this may lie in structural strain. Malcherek et al. (2001) constructed model equations to describe the effect of Mg–Fe mixing, and Na and H_2O contents as well, on the macroscopic shear strain in cordierite solid solutions. Their analysis shows that increasing Na, H_2O, and Mg contents reduce strain. They proposed that the scarcity of Fe-rich cordierites in nature and their restricted P–T stability field in phase equilibrium experiments reflects their greater structural distortion and strain.

Any deviation from linearity in Δ_{corr} has been described by the function $\delta(\Delta_{corr})$ – (e.g., Boffa Balllaran et al. 1999; Salje et al. 2000), and for the two high wavenumber regions it is equal to zero. (In the case of Fe^{2+}–Mg mixing in garnet, $\delta(\Delta_{corr}) = 0$ is also the case for these two wavenumber regions. Mg–Ca or Fe^{2+}–Ca mixing, on the other hand, gives rise to strong deviations from linear Δ_{corr} behavior). Hence, alkali-free Mg–Fe cordierite solid solutions should be characterized by relatively little structural heterogeneity and elastic strain energy gradients. In the low wavenumber region between 125 and 350 cm^{-1} the Δ_{corr} behavior is different and $\delta(\Delta_{corr}) > 0$ (Fig. 10). However, it should be stated that line broadening can also be a function of a number of factors including dynamic atomic disorder and magnetic-phonon interactions, for example (Geiger and Kolesov 2003). Mg–Fe garnets also show nonlinear Δ_{corr} behavior in the low wavenumber region that could be related to dynamic Fe/Mg-cation disorder in the large dodecahedral site. In the case of cordierite, high amplitude, low energy vibrations associated with the weakly bonded Na may be the cause. Armbruster (1986) measured large atomic displacement parameters for Na in cordierite and this is consistent with this hypothesis. It should be noted further that the Na vibrational behavior will also depend strongly on the neighboring H_2O configuration (Armbruster 1982; Kolesov and Geiger 2000). When Na is not bonded to H_2O (Class I), for example, it shows increased amplitude of vibration parallel to the channel direction. Low energy external vibrations of CO_2 and H_2O molecules in the channel cavities (Geiger and Kolesov 2003) could also possibly play a role in causing line broadening. Magnetic effects could possibly, in addition, be involved. There is strong line broadening observed in the Raman spectrum of fayalite that is attributed to phonon-magnetic exchange interactions (Geiger and Kolesov 2003). In order to investigate the possible contribution of these different effects to line broadening in the spectra of Mg–Fe cordierites, temperature-dependent spectroscopic measurements are required.

Energetics

The total energy of mixing of a system can be broken down into two parts, namely the elastic or strain energy and a chemical energy contribution (e.g., Srivastava et al. 1985; Ferreira et al. 1988). It is thought that elastic energies are generally more important in controlling the enthalpies of mixing, ΔH^{mix}, for most silicate solid solutions (Kerrick and Darken 1975; Greenwood 1979; Carpenter and Boffa Ballaran 2001; Geiger 2001), but other effects cannot be ignored. The elastic energy contribution is considered first. Recent HMIRS studies on different silicate structure types have shown for non-transition metal containing solid solutions such as jadeite–augite (diopside) (Boffa Ballaran et al. 1998), albite–anorthite (Atkinson et al. 1999), and pyrope–grossular (Boffa Ballaran et al. 1999) that a good correlation exists between line broadening behavior [i.e., $\delta(\Delta_{corr})$] and calorimetrically determined excess enthalpies of mixing. In all of these solid solutions mixing involves cations of relatively different sizes (e.g., Na–Si vs Ca–Al, Ca vs Mg) and positive excess enthalpies of mixing have been measured for two of them (Newton et al. 1977; Wood et al. 1980). The maximum excess enthalpy for jadeite–diopside is about 8.0 and 9.0 kJ/mol for grossular–pyrope. Octahedrally coordinated Fe^{2+} and Mg have similar ionic radii (0.78 vs 0.72 Å; Shannon 1976) and thus elastic strain gradients should be smaller in cordierite solid solutions and $\Delta H^{mix,\ elastic}$ should be small. This proposal is consistent with the observed $\delta(\Delta_{corr})$ behavior in the higher wavenumber regions (Fig. 10), but there are no calorimetric data on Mg–Fe cordierites to verify it. There are calorimetric ΔH^{mix} results on Mg–Fe mixing in three silicate solid solutions, namely the fayalite–forsterite (Wood and Kleppa 1981; Kojitani and Akaogi 1994), the enstatite–ferrosilite (Chatillon-Colinet et al. 1983), and the almandine–pyrope joins (Geiger et al. 1987). The fayalite–forsterite join has a maximum deviation from ideal mixing of about 2.5 kJ/mole, the enstatite–ferrosilite join about 2.0 kJ/mole, while the garnet binary has roughly 5.0 kJ/mole, although it should be stated that the errors and scatter in the calorimetric data are relatively large and ideal mixing behavior, $\Delta H^{mix} \approx 0$, can not be completely ruled out.

The chemical contribution(s) to the total enthalpy of mixing in cordierite is difficult to address completely. One contribution will come from the crystal field stabilization energy of Fe^{2+} in octahedral coordination. The electronic absorption spectrum of cordierite in the NIR contains two e_g-derived bands around 8,000 and 10,000 cm^{-1} arising from d-d electronic transitions from the ground state (Fig. 11). They shift to higher wavenumbers with increasing X_{Mg}. Their energies can be used to obtain the crystal field splitting (Δ_o) and the CFSE of Fe^{2+} as a function of composition using the different Mg–Fe cordierite spectra recorded by Khomenko et al. (2001). Burns (1993) discussed how CFSEs can affect the enthalpies of mixing and showed that they cannot be ideal in the case where the CFSE changes as a function of composition across, for example, a solid-solution binary. The octahedral M-site in cordierite has C2 point symmetry and it is compressed along a pseudo triad axis parallel to [001]. The d-orbital splitting in a monoclinic field is given in Burns (1993) and we take this as an appropriate description for the $^5T_{2g} \rightarrow {}^5E_g$ derived transition for Fe^{2+} in cordierite:

$$\mathrm{CFSE} = 2/5\Delta_o + \lambda \quad , \tag{3}$$

where Δ_o is the crystal field splitting and λ defines the baricenter of the lower split triplet level. The λ term cannot be measured directly, because the low energy electronic transitions occur in the (F)IR region where they are hidden under more intense lattice vibrations. A value of 240 cm^{-1} is assumed using the data in Burns (1993) and it is considered independent of composition. End member Mg cordierite has, of course, no CFSE and we determine the CFSE for end member Fe cordierite by extrapolating the energies of the two upper electronic states from the values of the intermediate Mg–Fe solid solutions. The excess ΔCFSEs for the different solid-solution compositions were calculated from:

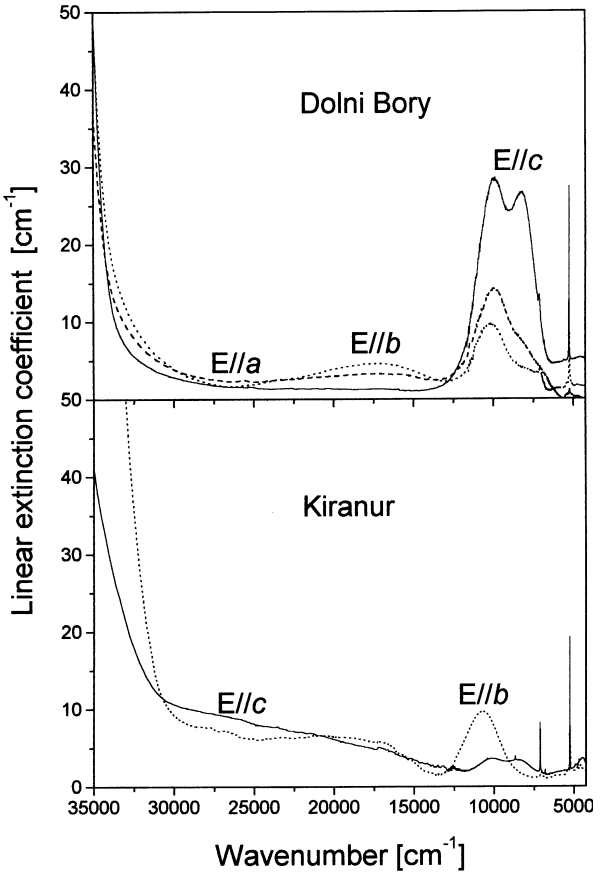

Fig. 11 Room temperature polarized optical absorption spectra of Fe-rich cordierite (Dolni Bory) no. 21 and the Mg-rich cordierite (Kiranur) no. 2 (from Geiger et al. 2002a). Note the two d-d electronic octahedral Fe^{2+} transitions at about 10,000 and 8,500 cm^{-1} as shown in the E//c spectra

$$\Delta CFSE^{excess} = CFSE(Mg - Fe - cord) - [CFSE(Mg - cord) + X_{Fe}CFSE(Fe - cord)]. \quad (4)$$

The resulting values across the binary are shown in Fig. 12. The data show a slight asymmetry with the largest nonideality of nearly −550 J/mol towards Fe cordierite. An asymmetric mixing model of the type:

$$\Delta CFSE^{excess} = X_{Fe}(1 - X_{Fe}) \cdot \left[W^{CFSE}_{Fe-Mg} + \left(W^{CFSE}_{Mg-Fe} - W^{CFSE}_{Fe-Mg}\right)X_{Fe}\right] \quad (5)$$

can describe the data, giving best-fit interaction parameters of $W^{CFSE}_{Fe\text{-}Mg} = -1.5$ (3) kJ/mol and $W^{CFSE}_{Mg\text{-}Fe} = -2.8$ (5) kJ/mol. The $\Delta CFSE^{excess}$ for cordierite are approximately the same as those observed for other Mg–Fe silicates with octahedral Fe^{2+}. They are roughly similar to those of $(Mg,Fe)_2SiO_4$ olivine solid solutions, for example, which have a maximum deviation of about −400 J/mole (Burns 1993). As in most solid solutions, they are negative and should act to stabilize the solid solution against any positive elastic energy due to strain.

The effect of additional components on cordierite's thermodynamic properties

Many natural cordierites are not strictly $(Mg, Fe)_2Al_4Si_5O_{18} \cdot x(H_2O, CO_2)$ solid solutions and it is a mistake in phase equilibrium calculations to always consider them as such. Many cordierites can be better described by the general formula $^{Ch}[Na, K]_y(Mg, Fe^{2+}, Mn^{2+}, Li)_2(Al, Be, Mg, Fe^{2+}, Fe^{3+})_4Si_5O_{18} \cdot x^{Ch}[H_2O, CO_2]$, with y and x < 1.0, and, hence, their thermodynamic properties could be affected by the presence of other components and we consider them briefly here. Molecules are often located in the small channel cavities. In alkali-free cordierites the effect of H_2O on structural heterogeneity and thus strain energies should be small to nonexistent. This is because Class I H_2O (Kolesov and Geiger 2000; Geiger and Kolesov 2003) has very weak interactions with the cordierite framework and is considered to be held in place by weak steric forces (Langer and Schreyer 1976; Winkler et al. 1994) and can be considered nearly "free" (Geiger and Kolesov 2003). This behavior is reflected further in the macroscopic volume measurements made on well characterized end member alkali-free H_2O-containing and H_2O-free cordierites that show no measurable differences between the two (Boberski and Schreyer 1990; Geiger and Voigtländer 2000). Class II H_2O bonds to the alkali atoms in the ring, and, is therefore not "free" and thus must be treated differently than Class I H_2O. It affects cordierite's framework properties indirectly through its interaction with the alkali cations in the six-membered tetrahedral rings (Armbruster 1982). In the case of CO_2, the degree of interaction with the framework should be small, in as much as its internal vibrations are not too different from those it posses in the free gaseous state (Kolesov and Geiger 2000), but more spectroscopic work is needed to quantify this aspect.

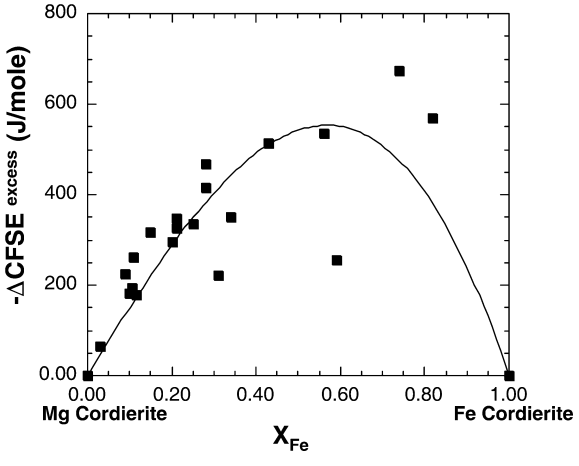

Fig. 12 Calculated excess CFSE (*solid squares*) for Fe^{2+} in Mg–Fe cordierite solid solutions. The *line* represents a least-squares asymmetric two-parameter fit to the data

The case for channel cations on structural heterogeneity and elastic energies is a different matter. Diffraction studies show that Na^+ in the six-membered rings interacts measurably with the oxygens of the tetrahedra (Armbruster 1982; Armbruster 1986). The formation of Na-O bonds draws the ring together, interacting especially with the underbonded oxygens that are shared between $Al_2$6 and Si_2l. It was shown that the different O-T-O angles in the ring decrease with increasing Na content. The effect that Na has on the energetics of cordierite is illustrated by the behavior of band E2 that has a large SiO_4 vibrational character (Fig. 6), for example, and whose wavenumber decreases slightly with increasing Na_2O content. More importantly, the presence of Na can produce line broadening in the high wavenumber region reflecting significant structural heterogeneity that will, in turn, affect measurably the thermodynamic behavior of cordierite. The effect of Na on structural heterogeneity can be greater than that related to Mg–Fe exchange. The results of Malcherek et al. (2001) indicate that Na makes a larger contribution (at least 6–7 times greater based on an atomic basis for the p.f.u.) to macroscopic strain than that arising from Mg–Fe exchange. For practical applications, for example in geothermobarometry calculations or in analyzing cordierite P–T phase relations, Na should not be ignored, nor should Class I and Class II H_2O be considered similar in terms of their thermodynamic behavior. It has been noted that there are difficulties in reconciling P–T phase relations based on results from synthetic Na-free cordierite versus those constructed from natural cordierite assemblages (Pattison et al. 2002) and further work in this area is needed.

Marked spectral changes are most apparent in the spectrum of the Na-rich cordierite no. 22 (Haddam, USA). Here the presence of both Be and Li may also

play a role in affecting the wavenumber systematics. Due to the lack of definite IR mode assignments for the internal tetrahedral vibrations, however, it is not possible to distinguish between effects which are caused by Be, affecting primarily $T_1$1, and which by Na, affecting the tetrahedra in the six-membered ring. The effects of Li and Be on the energetic properties of cordierite remain unknown. The slightly increased line broadening (Δ_{corr} values) observed for cordierite no. 2 (Kiranur) may also be related to small amounts of Fe^{2+} on $T_1$1 (0.02 cations p.f.u.; Geiger et al. 2000a). The presence of a large divalent cation in tetrahedral coordination should generate large local distortions, but its contribution to the total thermodynamics is probably small for most cordierites whose tetrahedral Fe contents are very low.

Acknowledgements We thank Tiziana Boffa Ballaran, Michael A. Carpenter, and Eckhard Salje for showing us the fine points of HMIRS. J. Vry, Th. Armbruster, A. Speer, P. Raase, and V. Khomenko generously provided cordierite samples. This work was supported by a grant, Ge 659/6-2, from the Deutsche Forschungsgemeinschaft. The comments of two anonymous reviewers and D.R.M. Pattison led to changes that improved significantly the manuscript. Professor J. Hoefs is thanked for his help in the review process.

References

Armbruster T (1982) Effect of H_2O on the structure of low-cordierite, a single crystal X-ray study. Proc 13th IMA General Meeting, Varna, Bulgaria, pp 485–503

Armbruster T (1985) Fe-rich cordierites from acid volcanic rocks, an optical and X-ray single-crystal structure study. Contrib Mineral Petrol 91:180–187

Armbruster T (1986) Role of Na in the structure of low-cordierite: a single-crystal X-ray study. Am Mineral 71:746–757

Armbruster T, Irouschek A (1983) Cordierites from the Lepontine Alps: Na + Be $\rightarrow$ Al substitution, gas content, cell parameters, and optics. Am Mineral 82:389–396

Atkinson AJ, Carpenter MA, Salje EKH (1999) Hard mode infrared spectroscopy of plagioclase feldspars. Eur J Mineral 11:7–23

Boberski C, Schreyer W (1990) Synthesis and water contents of Fe^{2+}-bearing cordierites. Eur J Mineral 2:565–584

Boffa Ballaran T, Carpenter MA, Domeneghetti MC, Salje EKH, Tazzoli V (1998) Structural mechanisms of solid solution and cation ordering in augite–jadeite pyroxenes. II: a microscopic perspective. Am Mineral 83:434–443

Boffa Ballaran T, Carpenter MA, Geiger CA, Koziol AM (1999) Local structural heterogeneity in garnet solid solutions. Phys Chem Miner 26:554–569

Burns RG (1993) Mineralogical applications of crystal field theory. Cambridge University Press, New York

Carpenter MA, Boffa Ballaran T (2001) The influence of elastic strain heterogeneities in silicate solid solutions. In: Geiger CA (ed) Solid solutions in silicate and oxide systems. European Notes in Mineralogy, vol 3, pp 155–178

Cerny P, Povondra P (1966) Beryllian cordierite from Vezna: (Na, K) + Be $\rightarrow$ Al. Neues Jahrb Mineral Monatsh 36–44

Chatillon-Colinet C, Newton RC, Perkins III D, Kleppa OJ (1983) Thermochemistry of $(Fe^{2+},Mg)SiO_3$ orthopyroxene. Geochim Cosmochim Acta 47:1597–1603

Ferreira LG, Mbaye AA, Zunger A (1988) Chemical and elastic effects on isostructural phase diagrams: the ϵ-G approach. Phys Rev B 37:10547–10570

Fuchs, LH (1969) Occurrence of cordierite and aluminous orthoenstatite in the Allende meteorite. Am Mineral 54:1645–1653

Geiger CA (2001) Thermodynamic mixing properties of binary oxide and silicate solid solutions determined by direct measurements: the role of strain. In: Geiger CA (ed) Solid solutions in silicate and oxide systems. European Notes in Mineralogy, vol 3, pp 71–100

Geiger CA, Kolesov BA (2003) Microscopic–macroscopic relationships in silicates: examples from IR and Raman spectroscopy and heat capacity measurements. In: Gramaccioli CM (ed) Energy modelling in minerals. European Notes in Mineralogy, vol 4, pp 347–387

Geiger CA, Voigtländer H (2000) The heat capacity of synthetic anhydrous Mg and Fe cordierite. Contrib Mineral Petrol 138:46–50

Geiger CA, Newton RC, Kleppa OJ (1987) Enthalpy of mixing of synthetic almandine-grossular and almandine-pyrope garnets from high-temperature solution calorimetry. Geochim Cosmochim Acta 51:1755–1763

Geiger CA, Winkler B, Langer K (1989) Infrared spectra of synthetic almandine-grossular and almandine-pyrope garnet solid solutions: evidence for equivalent site behavior. Mineral Mag 53:231–237

Geiger CA, Armbruster T, Khomenko V, Quartieri S (2000a) Cordierite I: the coordination of Fe^{2+}. Am Mineral 85:1255–1264

Geiger CA, Rager H, Czank M (2000b) Cordierite III: the coordination and concentration of Fe^{3+}. Contrib Mineral Petrol 140:344–352

Gibbs GV (1966) The polymorphism in cordierite I: the crystal structure of low cordierite. Am Mineral 51:1068–1087

Greenwood HJ (1979) Some linear and non-linear problems in petrology. Geochim Cosmochim Acta 43:1873–1885

Güttler B, Salje E, Putnis A (1989) Structural states of Mg cordierite III: infrared spectroscopy and the nature of the hexagonal-modulated transition. Phys Chem Miner 16:365–373

Hammonds KD, Dove MT, Giddy AP, Heine V, Winkler B (1996) Rigid-unit modes and structural phase transitions in framework silicates. Am Mineral 81:1057–1079

Hammonds KD, Bosenick A, Dove MT, Heine V (1998) Rigid unit modes in crystal structures with octahedrally coordinated atoms. Am Mineral 83:476–479

Hochella MF Jr, Brown GE Jr, Ross FK, Gibbs GV (1979) High-temperature crystal chemistry of hydrous Mg- and Fe-cordierite. Am Mineral 64:337–351

Kerrick DM, Darken LS (1975) Statistical thermodynamic models for ideal oxide and silicate solid solutions, with application to plagioclase. Geochim Cosmochim Acta 39:1431–1442

Khomenko V, Langer K, Geiger CA (2001) Structural allocation of iron ions in cordierite: spectroscopic study. Contrib Mineral Petrol 141:381–396

Kojitani H, Akaogi M (1994) Calorimetric study of olivine solid solutions in the system Mg_2SiO_4–Fe_2SiO_4. Phys Chem Miner 20:536–540

Kolesov BA, Geiger CA (2000) Cordierite II: the role of H_2O and CO_2. Am Mineral 85:1265–1274

Langer K, Schreyer W (1969) Infrared and powder x-ray diffraction studies on the polymorphism of cordierite, $Mg_2(Al_4Si_5O_{18})$. Am Mineral 54:1442–1459

Langer K, Schreyer W (1976) Apparent effects of molecular water on the lattice geometry of cordierite: a discussion. Am Mineral 61:1036–1040

Malcherek T, Domeneghetti MC, Tazzoli V, Ottolini L, McCammon C, Carpenter MA (2001) Structural properties of ferromagnesian cordierites. Am Mineral 86:66–79

Miyashiro A, Iiyama JT (1954) A preliminary note on a new mineral, indialite, polymorphic with cordierite. Imp Acad Jpn Proc 30:746–751

Mueller RF (1962) Energetics of certain silicate solid solutions. Geochim Cosmochim Acta 26:581–598

Newton RC (1966) BeO in pegmatitic cordierite. Mineral Mag 35:920–927

Newton RC, Charlu TV, Kleppa OJ (1977) Thermochemistry of high pressure garnets and clinopyroxenes in the system CaO–MgO–Al_2O_3–SiO_2. Geochim Cosmochim Acta 41:369–377

Pattison DRM, Spear FS, Debuhr CL, Cheney JT, Guidotti CV (2002) Thermodynamic modelling of the reaction muscovite + cordierite $\rightarrow$ Al_2SiO_5 + biotite + quartz + H_2O: constraints from natural assemblages and implications for the metapelitic petrogenetic grid. J Metamorph Geol 20:99–118

Pryce MW (1973) Low-iron cordierite in phlogopite schist from White Well, Western Australia. Mineral Mag 39:241–243

Salje EKH, Bismayer U (1997) Hard mode spectroscopy: the concept and applications. Phase Trans 63:1–75

Salje EKH, Carpenter MA, Malcherek T, Boffa Ballaran T (2000) Autocorrelation analysis of infrared spectra of minerals. Eur J Mineral 12:503–519

Schreyer W (1985) Experimental studies on cation substitutions and fluid incorporation in cordierite. Bull Mineral 108:273–291

Schreyer W, Maresch WV, Daniels P, Wolfsdorff P (1990) Potassic cordierites: characteristic minerals for high-temperature, very low pressure environments. Contrib Mineral Petrol 105:162–172

Shannon RD (1976) Revised effective ionic radii and systematic studies of interatomic distances in halides and chalcogenides. Acta Cryst A32:751–767

Srivastava GP, Martins JL, Zunger A (1985) Atomic structure and ordering in semiconductor alloys. Phys Rev B 31:2561–2564

Stanek J, Miskovsky J (1964) Iron-rich cordierite from the Dolni Bory pegmatite (in Czech). Cas Mineral Geol 9:191–192

Tarantino SC, Boffa Ballaran T, Carpenter MA, Domeneghetti MC, Tazzoli V (2002) Mixing properties of the enstatite–ferrosilite solid solution: II. A microscopic perspective. Eur J Mineral 14:537–547

Thompson AB (1976) Mineral reactions in pelitic rocks: I. Prediction of P–T–X (Fe–Mg) phase relations. Am J Sci 276:401–424

Wallace H, Wenk HR (1980) Structure variation in low cordierites. Am Mineral 65:96–111

White WB (1974) Order–disorder effects. In: Farmer VC (ed) The infrared spectra of minerals. Mineral Soc Great Britain, pp 87–110

Winkler B, Milman V, Payne MC (1994) Orientation, location, and total energy of hydration of channel H_2O in cordierite investigated by ab-initio total energy calculations. Am Mineral 79:200–204

Wood BJ, Kleppa OJ (1981) Thermochemistry of forsterite–fayalite olivine solid solutions. Geochim Cosmochim Acta 45:529–534

Wood BJ, Holland TJB, Newton RC, Kleppa OJ (1980) Thermochemistry of jadeite–diopside pyroxenes. Geochim Cosmochim Acta 44:1363–1371

Zhang M, Wruck B, Graeme Barber A, Salje EKH, Carpenter MA (1996) Phonon spectra of alkali feldspars: phase transitions and solid solutions. Am Mineral 81:92–104